

DONHEE LEE¹, DU HONG KANG¹, POONGYEON KIM¹, SI YOUNG CHANG^{1*}

SURFACE PROPERTIES OF ELECTROLYTIC POLISHED LAYER ON STS316L BY SINGLE MELTING AND DOUBLE MELTING

In this study, STS316L produced by a single-melting vacuum oxygen decarburization (VOD) process, referred to as SM, and a double-melting process involving vacuum induction melting (VIM) and vacuum arc remelting (VAR), referred to as DM, was subjected to extrusion and drawing to form a tube, followed by electrolytic polishing (EP). The surface roughness of layer on the DMed sample is 0.02 μm , which is much lower than that on the SMed sample of 0.13 μm . The thickness of the EP layer on STS316L by SM and DM revealed the values of approximately 7.1 nm and 8.2 nm, respectively. The Cr/Fe and CrO/FeO ratios in the EP layer on the DMed sample were 1.62 and 2.26, respectively, while, in the SMed sample, 1.22 and 2.03. Consequently, the EPed STS316L by DM showed better corrosion resistance in HCl solution and small amounts of Cr and Fe eluted in HCl solutions.

Keywords: Single melting; Double melting; Electrolytic polishing; STS316L; Corrosion resistance

1. Introduction

As the IT industry has grown, there has been a substantial increase in the number of manufacturing plants for semiconductors and the associated facilities and equipment. This growth has led to a higher demand for high-purity tubes with no contaminants, which are crucial for transporting highly corrosive gases used in semiconductor production lines [1-4]. Tubes and pipes used in the semiconductor industry must be extremely clean, and stainless steel is commonly used for this application. Specifically, 316L stainless steel (STS316L) is preferred due to its excellent corrosion resistance, which is attributed to its chemical composition, including 10-14% nickel and 16-18% chromium, slightly lower than STS304L [5-8]. Additionally, the thin oxide film (passive layer) composed of CrO and FeO on their surface serves as a protective barrier, preventing the underlying metals from reacting with corrosive elements like moisture and oxygen [9].

VOD, or Vacuum Oxygen Decarburization, is employed in the production of stainless steel tubes, specifically for reducing the carbon content in stainless steel tubes under a dual vacuum environment. Typically, using molten oxygen, it is employed to decrease the carbon content to a range of 0.01% to 0.02%, reaching the point where the final decarburization is achieved. This is essential because impurities of carbon and nitrogen in the steel, which need to be minimized for optimal toughness at normal

temperatures, are addressed during the VOD process [10-11]. And we refer to the VOD process as SM (Single Melting).

Melting processes have been reviewed extensively in the literature, with particular focus on vacuum induction melting (VIM) and vacuum arc remelting (VAR) [12-14]. Vacuum induction melting (VIM) utilizes high purity gas to evaluate and improve the quality and the contamination levels of final ingots. VIM helps to smoothen the surface and improve alloy homogeneity, thanks to the inherent stirring action of the induction field and precise control of melt superheat [15-18]. Vacuum arc remelting (VAR) process is a refining method used as secondary processing for the homogenization of high melting point and oxygen sensitive materials, such as seamless tube used in semiconductor manufacturing. It involves melting the material under vacuum conditions, which helps to remove impurities and reduce porosity in the ingots. And we refer to the VIM-VAR process as DM (Double Melting) [19-21].

Electrolytic polishing (EP) is widely used in many areas related to the semiconductor, medical, ultra-clean gas, etc. EP produces excellent results when the polished inside surfaces of tubes and pipes contact with a pure gas. The performance of semiconductor depends on the purity of gas through the STS316L tubes. Inner surface of stainless steel is required to not only decrease the surface roughness value but also improve corrosion resistance by removing the damaged layer and impurities related

¹ KOREA AEROSPACE UNIVERSITY, DEPARTMENT OF MATERIALS SCIENCE AND ENGINEERING, GOYANG, KOREA

* Corresponding author: sychang@kau.ac.kr



to the corrosion of surface. Electrolytic polishing is considered as the most effective machining technique to achieve these requirements [19-23].

Therefore, the objective in this study is to investigate the surface properties of the electrolytic polished layer on STS316L produced by SM and DM.

2. Experimental

In this study, STS316L samples produced by SM and DM processes were used. The composition of the SMed and DMed samples is shown in TABLE 1. The DMed sample showed particularly reduced levels of carbon (C), silicon (Si), manganese (Mn) and sulfur (S) compared to the SMed sample.

After melting the STS316L using both methods, the material underwent extrusion and drawing processes, followed by heat treatment at 1258 K for one hour to produce 1/4 inch inner diameter tubes. The tubes were subsequently subjected to electrolytic polishing. For this, the tubes were electrolytically polished using mixed solution of H_3O_4P (Phosphoric acid), H_2SO_4 (Sulfuric acid) and DI (distilled water) in a 6:3:1 ratio.

The microstructure was observed by optical microscope (OM). Also, the surface roughness (R_a) was measured through a surface profilometer. The thickness of electrolytic polished layer was measured by auger electron spectroscopy (AES, PHI 700Xi) with 0.47 nm/min in sputtering rate. Cr/Fe and CrO/FeO ratios were calculated with equation previously reported through X-ray photoelectron spectroscopy (XPS, Thermo VG) [24]. Corrosion test was conducted by immersing in 40% HCl solution to measure the relative weight loss. The corrosion stability was evaluated by the eluted ions immersed in 40% HCl for 24 hr.

3. Results and discussion

Fig. 1 shows the microstructure of STS316L produced by SM and DM before/after EP. The grain sizes of STS316L produced by SM and DM without EP were approximately 60 μm and 55 μm , respectively. After EP, the grain sizes were 62 μm for SM and 57 μm for DM, indicating a distinct difference in grain size by EP. However, there was a distinct difference between the SMed and DMed samples.

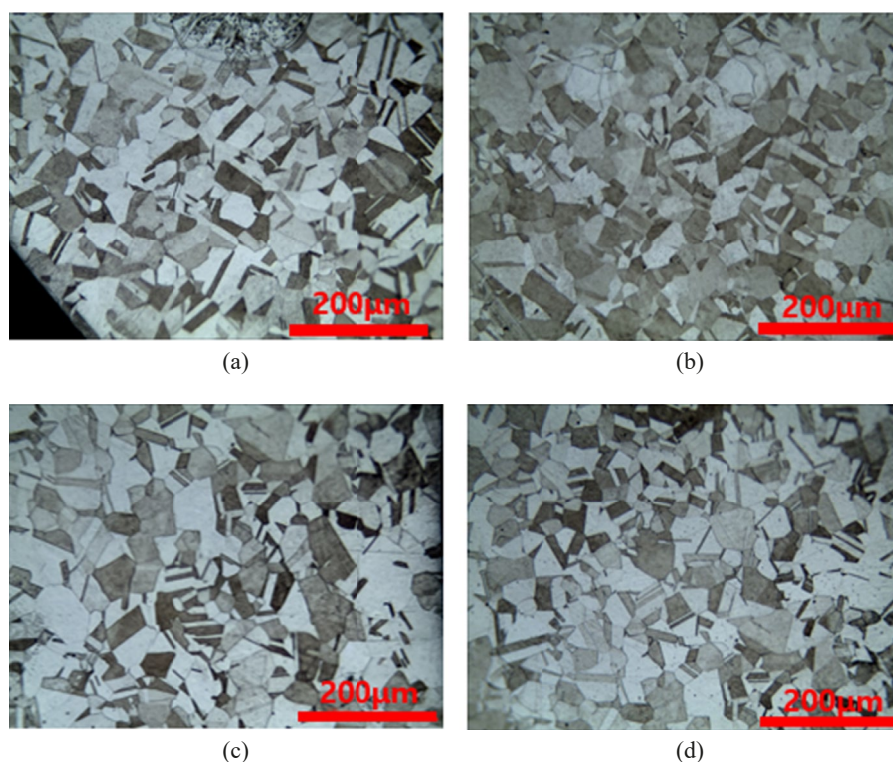


Fig. 1. Microstructures of STS316L: (a) SM, (b) DM, (c) SM-EP and (d) DM-EP

TABLE 1

Chemical compositions of STS316L produced by SM and DM

	wt. %												
	C	Si	Mn	P	S	Cu	N	Cr	Mo	Al	O	N	Fe
ASTM 316L	0.03	1.00	2.00	0.045	0.030	—	10.0-14.0	16.0-18.0	2.0-3.0	—	—	1.0	Bal.
SM	0.015	0.18	0.05	<0.001	0.015	0.25	15.03	16.85	3.02	<0.01	0.001	0.001	Bal.
DM	0.007	0.13	0.02	<0.001	0.002	0.14	14.78	16.64	2.26	<0.01	0.0008	0.0008	Bal.

Fig. 2 presents the surface roughness of the EP layers on SM and DM samples. For the SMed sample, the surface roughness was $0.131\text{ }\mu\text{m}$, while the DMed sample, showed $0.021\text{ }\mu\text{m}$.

Fig. 3 shows the analysis results of EP layer on STS316L by AES. The thickness was obtained by multiplying the sputter time with the sputter rate at a half of maximum intensity of oxygen. The thickness of the EP layer on STS316L was approximately 7.1 nm for SM and 8.2 nm for DM. On the other hand, the Cr/Fe and CrO/FeO ratios calculated from the XPS result [24] were 1.62 and 2.26 in the DMed sample, respectively, while the SMed

sample displayed lower ratios of 1.22 and 2.03, illustrating enhanced ratios in the DMed sample.

Fig. 4(a) presents the corrosion test results according to exposure time in HCl solution. After 168 hours, the DMed STS316L showed the weight loss of 0.28 g , indicating better corrosive resistance compared to the SM, which experienced a weight loss of 0.35 g . After EP, the weight loss for DM was 0.1 g , which reveals significant reduction compared to 0.23 g for SM. This indicates that the EP treatment for the DMed STS316L much effectively minimizes corrosion compared to the SMed sample.

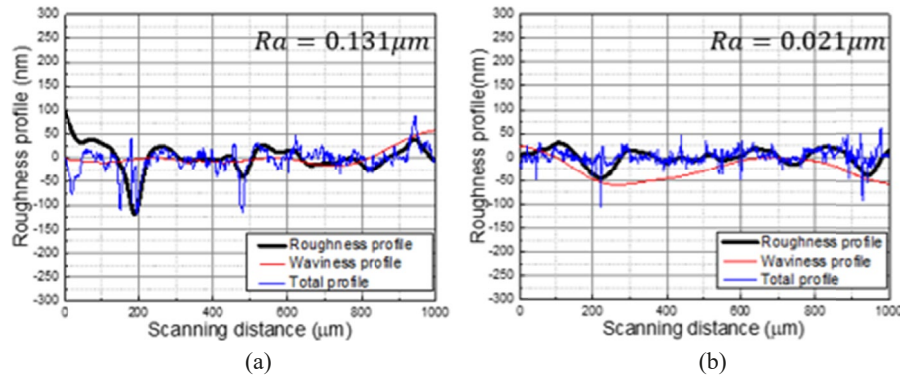


Fig. 2. Surface roughness of EP layer on STS316L: (a) SM and (b) DM

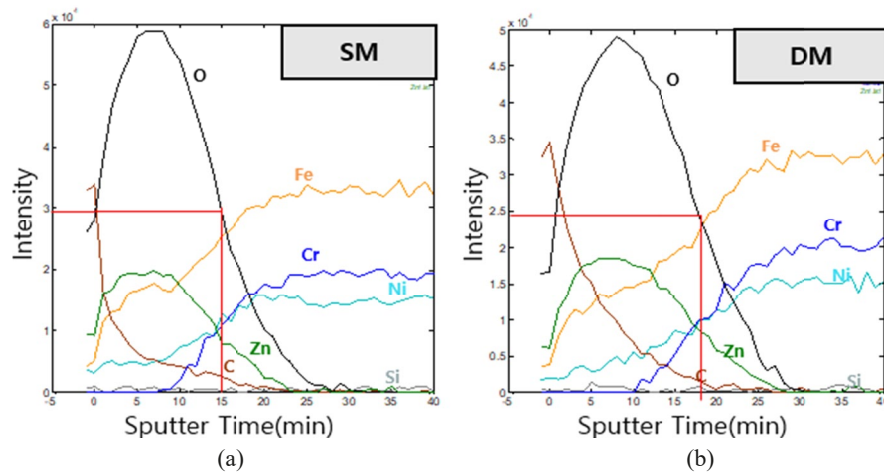


Fig. 3. Analysis of EP Layer on STS316L: (a) SM and (b) DM

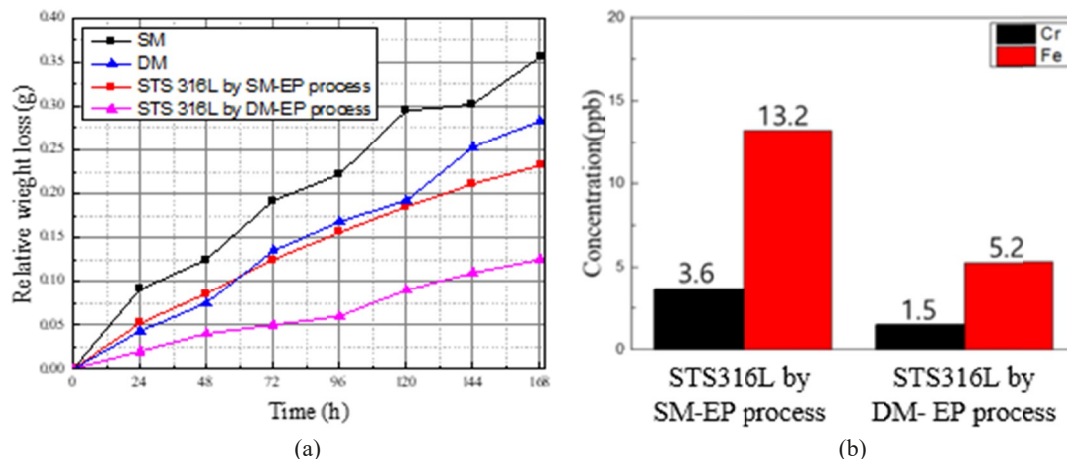


Fig. 4. (a) Weight loss and (b) eluted ions of EPed STS316L immersed in 40 wt.% HCl

In addition, the corrosion stability of STS316L was evaluated by measuring the concentration (ppb) of ions eluted in the HCl solution as shown in Fig. 4(b). There was a significant difference in concentration between the EPed samples by SM and DM. The concentration of eluted Cr ion was 1.5 ppb in the DMed sample and 3.6 ppb in the SMed sample. There was a notable difference in the eluted amount of Fe ion as well, with 5.2 ppb and 13.2 ppb in the SMed and DMed samples, respectively.

By applying the DM, the grains become small (Fig. 1) and the contents of C, Si, Mn and S elements are reduced (TABLE 1). In general, the smaller grains, the faster diffusion through grain boundary. And also, the reduced Mn and S contents by DM result in the decrease of Mn fume and the widen bead during welding of stainless steel [25]. On the other hand, low carbon concentration restrains the formation of chromium carbide (CrC), which increases the available chromium oxide on the surface, potentially raising the Cr/Fe and CrO/FeO ratios [26]. Additionally, the reduction of Si content caused to the restrained formation of silicon oxide, indicating the promoted formation of chrome oxide [27]. Accordingly, it is reasonably considered that the reason why the EPed STS316L by DM shows better corrosion resistance is due to the preferred formation of stable chrome oxide by diffusion through the increased grain boundary and reduction of C and Si contents in the DMed STS316L.

4. Conclusions

The STS316L obtained through a single-melting (VOD) and a double-melting (VIM, VAR) and subsequently extrusion, drawing electrolytically polished (EP). And then the surface properties of the EPed layer were investigated.

The DM resulted in the decreased contents of Si, C, compared to the SMed STS316L. The grain sizes of STS316L by SM and DM without EP were approximately 60 and 55 μm , respectively, with no difference found after EP. The DMed sample had the surface roughness of layer of 0.02 μm , which was lower than that on the SMed sample. The thickness of layer was 7.1 and 8.2 nm in the SMed and DMed samples, respectively. In the DMed sample, the ratios of Cr/Fe and CrO/FeO were 1.62 and 2.26, while the SMed sample showed much lower ratios of 1.22 and 2.03. After being immersed in HCl for 168h, the weight losses were 0.35g and 0.28g in the SMed and DMed samples, respectively. And also, much smaller amounts of Cr and Fe were eluted from the EPed STS316L by DM compared to SM.

Acknowledgments

This work was supported by the Ministry of Trade, Industry and Energy (MOTIE, Korea) under Industrial Technology Innovation Program, No.20009937.

REFERENCES

- [1] E. Krapf, R. Preisser, *Process Technology of Water Treatment*, Springer (1988).
- [2] C.-W. Shen, P.P. Tran, P.T.M. Ly, *Sustainability* **10**, 1545-1567 (2018).
- [3] K.H. Kim, B.Y. Cho, *J. Kor. Surf. Eng.* **41**, 38-42 (2008).
- [4] J.B. Lee, *Mater. Chem. Phys.* **99**, 224-234 (2006).
- [5] T.M.L. Pham, *Sustainability* **10**, 1545-1567 (2018).
- [6] K. Rokosz, T. Hryniewicz, S. Rzakiewicz, S. Raaen, *Technical Gazette* **22**, 415-424 (2015).
- [7] S.K. Jang, M.S. Han, S.J. Kim, *Trans. Nonferrous Met. Soc. China*, **19**, 930-934 (2009).
- [8] S.Y. Song, D.W. Lee, D.V. Cong, *J. Powder Mater.* **29**, 14-21 (2022).
- [9] Z. Wang, E.-M. Paschalidou, A. Seyeux, S. Zanna, V. Maurice, P. Marcus, *Frontiers in Materials* **6**, 232 (2019).
- [10] R. Ding, B. Blanpain, P. Jones, P. Wollants, *Metall. Mater. Trans. B*, **31**, 197-206 (2000).
- [11] X. Yingtie, C. Zhaoping, Z. Ge, *Metall. Mater. Trans. B*, **40**, 345-352 (2009).
- [12] A.R. Pelton, D. Stoeckel, T.W. Duerig, *Mater. Sci. Forum.* **327-328** (2000).
- [13] M.H. Wu, *Mater. Sci. Forum.* **394-395** (2002).
- [14] L.M. Wang, L.H. Liu, H. Yang, L.Y. Wang, G.Q. Xiu, *Mater. Sci. Forum.* **394-395**, 297-300 (2002).
- [15] J. Frenzel, Z. Zhang, K. Neuking, G. Eggeler, *Alloys and Compounds* **385**, 214-223 (2004).
- [16] J. Otubo, O.D. Rigo, C. Moura Neto, P.R. Mei, *Mater. Sci. Eng. A*, 438-440, 679-682 (2006).
- [17] K. Kamysnykova, J. Lapin, *Vacuum* **154**, 218-226 (2018).
- [18] N.M. Griesenauer, S.R. Lyon, C.A. Alexander, *J. Vac. Sci. Technol. A/B*, **9**, 1351-1355 (1972).
- [19] P. Lochynski, A. Sikora, B. Szczygiel, *Surf. Eng.* **33**, 395-403 (2017).
- [20] K. Rokosz, J. Lahtinen, T. Hryniewicz, S. Rzakiewicz, *Surf. Coat. Technol.* **276**, 516-520 (2015).
- [21] P. Lochynski, M. Kowalski, B. Szczygiel, K. Kuczewski, *Pol. J. Chem. Technol.* **18**, 76-81 (2016).
- [22] S.W. An, J.H. Lee, M.S. Park, *J. Korean Soc. Manuf. Process. Eng.* **3**, 52-57 (2004).
- [23] M. Oravcová, P. Palček, V. Zatkalíková, T. Tański, M. Król, *Mater. Sci. Eng.* **175**, 1-6 (2017).
- [24] H. Lee, G. Kim, G. Kim, S. Chang, *J. Korean Foundry Soc.* **43**, 223-229 (2023).
- [25] I. Cameron, *Proc. ASME Int. Pipeline Conf.* **45141**, 501-512 (2012).
- [26] R. Zhang, W. Yan, P. Jin, Y. Liu, X. Zhou, *J. Mater. Sci.* **57**, 19327-19337 (2022).
- [27] J. L. Qiao, F.H. Guo, S. T. Qiu, et al. *J. Iron Steel Res. Int.* **28**, 327-334 (2021).